Angular trispectrum of the cosmic microwave background

Wayne Hu
5640 South Ellis Avenue, University of Chicago, Chicago, Illinois 60637
(Received 23 April 2001; published 11 September 2001)

We study the general properties of the cosmic microwave background temperature four-point function, specifically its harmonic analogue, the angular trispectrum, and illustrate its utility in finding optimal quadratic statistics through the weak gravitational lensing effect. We determine the general form of the trispectrum, under the assumptions of rotational, permutation, and parity invariance, its estimators on the sky, and their Gaussian noise properties. The signal-to-noise in the trispectrum can be highly configuration dependent and any quadratic statistic used to compress the information to a manageable two-point level must be carefully chosen. Through a systematic study, we determine that for the case of lensing a specific statistic, the divergence of a filtered temperature-weighted temperature-gradient map contains the maximal signal-to-noise and reduces the variance of estimates of the large-scale convergence power spectrum by over an order of magnitude over previous gradient-gradient techniques. The total signal-to-noise for lensing with the Planck satellite is of order 60 for a fiducial cold dark matter model with a cosmological constant (ΛCDM).

DOI: 10.1103/PhysRevD.64.083005 PACS number(s): 98.70.Vc

I. INTRODUCTION

The power spectra or two-point correlations of cosmic microwave background (CMB) temperature and polarization anisotropies are widely recognized as a gold mine of information on cosmology. These spectra in fact contain all of the information embedded in the CMB if the underlying fluctuations are Gaussian distributed. Nonetheless even if the initial density fluctuations are Gaussian, non-Gaussianity in the CMB temperature fluctuations will be generated by nonlinear processes. These generally are associated with the secondary anisotropies that are imprinted as the photons propagate through the large-scale structure of the Universe from the epoch of recombination.

Secondary signatures in the three-point correlation of temperature anisotropies have recently received much attention [1–3] following early pioneering work on intrinsic correlations in the initial conditions [4,5]. The four-point correlation and its harmonic analogue, the trispectrum, has received considerably less attention despite the fact that it directly controls the noise properties of the estimators of the power spectrum. In particular, an all-sky treatment of the trispectrum that incorporates the full rotational symmetry properties of the trispectrum has been lacking in the literature (cf. Ref. [6]). Exploitation of the symmetry properties can assist in the isolation of the physical mechanisms underlying the generation of the trispectrum, as we shall see.

In this paper, we establish the framework needed to study the trispectrum on the full sky. We begin in Sec. II with a discussion of the symmetry properties of the *n*-point function on the sky, with an emphasis on the four-point function, and their implications for the general form of the harmonic spectra. We consider estimators of the trispectrum and their noise properties in Sec. III, and the trispectrum-based power spectra of quadratic statistics in Sec. IV. Calculational techniques and relationships to the flat-sky formalism are given in two Appendixes. In Sec. V, we consider the specific case of the trispectrum generated by weak gravitational lensing of CMB photons by the large-scale structure of the Universe and show that there exists a quadratic statistic that optimally recovers the projected gravitational potential power spectrum (or convergence) on large scales. We conclude in Sec. VI.

II. SYMMETRIES

In this section, we derive the requirements that rotational, permutation, and parity symmetry impose on the $n=$(two, three, four)-point correlation functions on the sphere and their spherical harmonic analogues: the power spectrum, bispectrum, and trispectrum. We begin with general considerations for the *n*-point function in Sec. II A, review the implications for the power spectrum and bispectrum in Sec. II B, and derive the consequences for the trispectrum in Sec. II C. In Sec. II D, we show how to construct trispectra with the required symmetry properties.

A. General considerations

We begin by requiring statistical isotropy of the *n*-point correlation function on the sphere and its harmonic analogue,

$$\langle \Theta(\hat{\mathbf{n}}_1)\cdots\Theta(\hat{\mathbf{n}}_n)\rangle = \sum_{l_1\cdots l_n}\sum_{m_1\cdots m_n}\langle \Theta_{l_1m_1}\cdots\Theta_{l_nm_n}\rangle \times Y^{m_1}_{l_1}(\hat{\mathbf{n}}_1)\cdots Y^{m_n}_{l_n}(\hat{\mathbf{n}}_n). \quad (1)$$

Statistical isotropy demands that the *n*-point function is invariant under an arbitrary rotation R whose action on a spherical harmonic is expressed in terms of the Wigner-D function,

$$R[Y^m_l(\hat{\mathbf{n}})] = \sum_{m'} D^l_{m'm}(\alpha,\beta,\gamma)Y^{m'}_l(\hat{\mathbf{n}}), \quad (2)$$

where α, β, and γ are the Euler angles of the rotation. To satisfy rotational invariance the harmonics must obey the relation

$$\langle \Theta_{l_1 m_1} \cdots \Theta_{l_n m_n} \rangle = \sum_{m_1' \cdots m_n'} \langle \Theta_{l_1 m_1'} \cdots \Theta_{l_n m_n'} \rangle \times D^{l_1}_{m_1 m_1'} \cdots D^{l_n}_{m_n m_n'}, \quad (3)$$

for all α, β, and γ. The reduction of this relation proceeds as follows. Each pair of rotation matrices may be coupled into a single rotation via the group multiplication property (or equivalently the addition of angular momentum),

$$D^{l_1}_{m_1 m_1'} D^{l_2}_{m_2 m_2'} = \sum_{LMM'} \begin{pmatrix} l_1 & l_2 & L \\ m_1 & m_2 & -M \end{pmatrix} \begin{pmatrix} l_1 & l_2 & L \\ m_1' & m_2' & -M' \end{pmatrix} \times (2L+1)(-1)^{M+M'} D^L_{MM'}. \quad (4)$$

When the product is reduced to a pair of D matrices, one seeks the form of the harmonic n-point function that reduces the pair to the orthogonality condition for rotations

$$\sum_m (-1)^{m_2 - m} D^{l_1}_{m_1 m} D^{l_1}_{-m_2 - m} = \delta_{m_1 m_2}, \quad (5)$$

which is valid for an arbitrary rotation. The indices can then be permuted to find alternate orderings of the pairings.

Invariance under a parity transformation which takes $\hat{\mathbf{n}} \to -\hat{\mathbf{n}}$,

$$Y_l^m \to (-1)^l Y_l^m, \quad (6)$$

would require that

$$\sum_{i=1}^n l_i = \text{even}. \quad (7)$$

Reality of the underlying Θ field and the fact that

$$Y_l^m{}^* = (-1)^m Y_l^{-m}, \quad (8)$$

requires that

$$\Theta_l^m{}^* = (-1)^m \Theta_l^{-m}. \quad (9)$$

B. Power spectrum and bispectrum

For the two-point function there is only one step. The reduction of Eq. (5) requires the form

$$\langle \Theta_{l_1 m_1} \Theta_{l_2 m_2} \rangle = \delta_{l_1 l_2} \delta_{m_1 - m_2} (-1)^{m_1} C_{l_1}. \quad (10)$$

For the three-point function one first collapses one product of rotation matrices leaving

$$\langle \Theta_{l_1 m_1} \cdots \Theta_{l_3 m_3} \rangle = \sum_{m_1' \cdots m_3'} \langle \Theta_{l_1 m_1'} \cdots \Theta_{l_3 m_3'} \rangle \sum_{LMM'} (2L+1) \times (-1)^{M+M'} \begin{pmatrix} l_1 & l_2 & L \\ m_1 & m_2 & -M \end{pmatrix} \times \begin{pmatrix} l_1 & l_2 & L \\ m_1' & m_2' & -M' \end{pmatrix} D^L_{MM'} D^{l_3}_{m_3 m_3'}. \quad (11)$$

In order to reduce this relation to the orthogonality condition Eq. (5), the sum over m' of the three-point function must be proportional to $\delta_{L l_3} \delta_{M' - m_3'}$. Recalling the identity

$$\sum_{m_1 m_2} \begin{pmatrix} l_1 & l_2 & L \\ m_1 & m_2 & M \end{pmatrix} \begin{pmatrix} l_1 & l_2 & L' \\ m_1 & m_2 & M' \end{pmatrix} = \frac{\delta_{LL'} \delta_{MM'}}{2L+1}, \quad (12)$$

we can obtain the desired relation if the m dependence of the three-point function obeys

$$\langle \Theta_{l_1 m_1} \cdots \Theta_{l_3 m_3} \rangle = \begin{pmatrix} l_1 & l_2 & l_3 \\ m_1 & m_2 & m_3 \end{pmatrix} B_{l_1 l_2 l_3}. \quad (13)$$

C. Trispectrum

The form of the four-point function follows the same steps except that we use the group multiplication properties to pair say (l_1, l_2) and (l_3, l_4) leading to the condition

$$\langle \Theta_{l_1 m_1} \cdots \Theta_{l_4 m_4} \rangle = \sum_{m_1' \cdots m_4'} \sum_{L_{12} M_{12} M_{12}'} (2L_{12}+1) \times (-1)^{M_{12} + M_{12}'} \begin{pmatrix} l_1 & l_2 & L_{12} \\ m_1 & m_2 & -M_{12} \end{pmatrix} \times \begin{pmatrix} l_1 & l_2 & L_{12} \\ m_1' & m_2' & -M_{12}' \end{pmatrix} D^{L_{12}}_{M_{12} M_{12}'} \times \sum_{L_{34} M_{34} M_{34}'} (2L_{34}+1) \times (-1)^{M_{34} + M_{34}'} \begin{pmatrix} l_3 & l_4 & L_{34} \\ m_3 & m_4 & -M_{34} \end{pmatrix} \times \begin{pmatrix} l_3 & l_4 & L_{34} \\ m_3' & m_4' & -M_{34}' \end{pmatrix} D^{L_{34}}_{M_{34} M_{34}'} \times \langle \Theta_{l_1 m_1'} \cdots \Theta_{l_4 m_4'} \rangle. \quad (14)$$

The same reasoning that led to the choice of the form of the three-point function implies that the following form is a solution:

$$\langle \Theta_{l_1 m_1} \cdots \Theta_{l_4 m_4} \rangle = \sum_{LM} \begin{pmatrix} l_1 & l_2 & L \\ m_1 & m_2 & -M \end{pmatrix} \begin{pmatrix} l_3 & l_4 & L \\ m_3 & m_4 & M \end{pmatrix} \times (-1)^M Q^{l_1 l_2}_{l_3 l_4}(L). \quad (15)$$

Geometrically, $Q^{l_1 l_2}_{l_3 l_4}(L)$ represents a quadrilateral composed of sides with length $l_1 \cdots l_4$. The index L represents one of the diagonals of the quadrilateral and is also the shared third side of the two triangles formed by the corresponding pairs of sides. The Wigner-3j symbols in Eq. (15) ensure that the

triangle inequalities are satisfied. For this reason we will often refer to a set (l_1,l_2,l_3,l_4,L) as a given "configuration" of the quadrilateral.

The two other unique pairings of the indices, (l_1,l_3) and (l_1,l_4), yield alternate representations of the four-point function. These are not independent since all three couplings yield complete sets according to the theory of the addition of angular momenta. The alternate representations are constructed as linear combinations of the (l_1,l_2) representation with weights given by the Wigner-6j recoupling coefficients (see Appendix A),

$$Q^{l_1 l_3}_{l_2 l_4}(L)=\sum_{L'}(-1)^{l_2+l_3}(2L+1)\begin{Bmatrix} l_1 & l_2 & L' \\ l_4 & l_3 & L \end{Bmatrix} Q^{l_1 l_2}_{l_3 l_4}(L'),$$

$$Q^{l_1 l_4}_{l_3 l_2}(L)=\sum_{L'}(-1)^{L+L'}(2L+1)\begin{Bmatrix} l_1 & l_2 & L' \\ l_3 & l_4 & L \end{Bmatrix} Q^{l_1 l_2}_{l_3 l_4}(L'), \tag{16}$$

where we have used Eq. (A4) to project one coupling scheme onto another.

Symmetry with respect to the $4!/3=8$ remaining permutations (two orderings of the pairs, four orderings within the pairs) requires that

$$Q^{l_1 l_2}_{l_3 l_4}(L)=(-1)^{\Sigma_U}Q^{l_2 l_1}_{l_3 l_4}(L)=(-1)^{\Sigma_L}Q^{l_1 l_2}_{l_4 l_3}(L)=Q^{l_3 l_4}_{l_1 l_2}(L), \tag{17}$$

where $\Sigma_U=l_1+l_2+L$ and $\Sigma_L=l_3+l_4+L$. If the four-point function is parity invariant then

$$Q^{l_1 l_2}_{l_3 l_4}(L)=Q^{l_2 l_1}_{l_4 l_3}(L). \tag{18}$$

We shall show how to construct trispectra that obey these properties in the next section.

Finally it is useful to separate the contributions from the unconnected or Gaussian piece and the connected or trispectrum piece

$$Q^{l_1 l_2}_{l_3 l_4}(L)=G^{l_1 l_2}_{l_3 l_4}(L)+T^{l_1 l_2}_{l_3 l_4}(L), \tag{19}$$

where

$$G^{l_1 l_2}_{l_3 l_4}(L)=(-1)^{l_1+l_3}\sqrt{(2l_1+1)(2l_3+1)}C_{l_1}C_{l_3}\delta_{l_1 l_2}\delta_{l_3 l_4}\delta_{L0} + (2L+1)C_{l_1}C_{l_2}[(-1)^{l_2+l_3+L}\delta_{l_1 l_3}\delta_{l_2 l_4} + \delta_{l_1 l_4}\delta_{l_2 l_3}]. \tag{20}$$

D. Enforcing symmetries

The symmetries of the trispectrum described above may be enforced by the following construction. First we describe the four-point function by a form that is explicitly symmetric in the three unique pairings,

$$\langle\Theta_{l_1 m_1}\cdots\Theta_{l_4 m_4}\rangle_c=\sum_{LM}P^{l_1 l_2}_{l_3 l_4}(L)\begin{pmatrix} l_1 & l_2 & L \\ m_1 & m_2 & -M \end{pmatrix} \times\begin{pmatrix} l_3 & l_4 & L \\ m_3 & m_4 & M \end{pmatrix}(-1)^M+(l_2\leftrightarrow l_3) +(l_2\leftrightarrow l_4), \tag{21}$$

where c denotes the fact that we have removed the Gaussian piece of Eq. (20). The two latter pairings can be projected onto the (l_1,l_2) basis with the help of the Wigner-6j symbol to give

$$T^{l_1 l_2}_{l_3 l_4}(L)=P^{l_1 l_2}_{l_3 l_4}(L)+(2L+1)\sum_{L'}\Bigg[(-1)^{l_2+l_3} \times\begin{Bmatrix} l_1 & l_2 & L \\ l_4 & l_3 & L' \end{Bmatrix}P^{l_1 l_3}_{l_2 l_4}(L')+(-1)^{L+L'} \times\begin{Bmatrix} l_1 & l_2 & L \\ l_3 & l_4 & L' \end{Bmatrix}P^{l_1 l_4}_{l_3 l_2}(L')\Bigg]. \tag{22}$$

Within the three unique pairings, there are four permutations of the ordering implying that P is constructed as

$$P^{l_1 l_2}_{l_3 l_4}(L)=\mathcal{T}^{l_1 l_2}_{l_3 l_4}+(-1)^{\Sigma_U}\mathcal{T}^{l_2 l_1}_{l_3 l_4}+(-1)^{\Sigma_L}\mathcal{T}^{l_1 l_2}_{l_4 l_3} +(-1)^{\Sigma_U+\Sigma_L}\mathcal{T}^{l_2 l_1}_{l_4 l_3}. \tag{23}$$

The reduced function $\mathcal{T}$ underlying the trispectrum is an arbitrary function of its arguments except that it must be symmetric against exchange of its upper and lower indices

$$\mathcal{T}^{l_1 l_2}_{l_3 l_4}(L)=\mathcal{T}^{l_3 l_4}_{l_1 l_2}(L), \tag{24}$$

and if parity invariant obeys

$$\mathcal{T}^{l_1 l_2}_{l_3 l_4}(L)=\mathcal{T}^{l_2 l_1}_{l_4 l_3}(L). \tag{25}$$

This then completes the enforcing of the rotation, permutation and parity symmetries of the trispectrum.

III. ESTIMATORS AND SIGNAL-TO-NOISE

We show in Sec. III A that the fundamental estimator of the trispectrum involves a weighted sum over the multipole moments in a given quadruplet of harmonics. These estimators have well defined noise properties as derived in Sec. III B which can be used to calculate the theoretical signal-to-noise in the trispectrum. A nonvanishing trispectrum can on the other hand decrease the signal-to-noise in the power spectrum by introducing a covariance between its estimators as shown in Sec. III C.

A. Estimators

From the orthogonality properties of the Wigner-3j symbol, one can invert the relationship for the four-point spectrum to form the estimator

$$\hat{T}^{l_1 l_2}_{l_3 l_4}(L) = (2L+1) \sum_{m_1 m_2 m_3 m_4 M} (-1)^M \begin{pmatrix} l_1 & l_2 & L \\ m_1 & m_2 & M \end{pmatrix} \times \begin{pmatrix} l_3 & l_4 & L \\ m_3 & m_4 & -M \end{pmatrix} \langle \Theta_{l_1 m_1} \cdots \Theta_{l_4 m_4} \rangle - \hat{G}^{l_1 l_2}_{l_3 l_4}, \tag{26}$$

where the estimator for the Gaussian piece is constructed out of those for the power spectrum. Note that for configurations whose l sides are not equal in pairs, the Gaussian piece vanishes and the sum over m's of the spherical harmonic coefficients is an unbiased estimator of the trispectrum.

We can alternately form an estimator of particular configurations of the trispectrum directly from the sky map itself without an explicit expansion in spherical harmonics. Following Spergel and Goldberg [8], let us define a new set of sky maps weighted in rings centered around a point $\hat{\mathbf{q}}$:

$$e_l(\hat{\mathbf{q}}) = \sqrt{\frac{2l+1}{4\pi}} \int d\hat{\mathbf{n}} \Theta(\hat{\mathbf{n}}) P_l(\hat{\mathbf{n}} \cdot \hat{\mathbf{q}}). \tag{27}$$

Expanding the Wigner-3j symbols in terms of spherical harmonics and using the addition theorem, we obtain

$$\begin{pmatrix} l_1 & l_2 & L \\ 0 & 0 & 0 \end{pmatrix} \begin{pmatrix} l_3 & l_4 & L \\ 0 & 0 & 0 \end{pmatrix} [\hat{T}^{l_1 l_2}_{l_3 l_4}(L) + \hat{G}^{l_1 l_2}_{l_3 l_4}(L)] = (2L+1) \int \frac{d\hat{\mathbf{q}}_a}{4\pi} \int \frac{d\hat{\mathbf{q}}_b}{4\pi} e_{l_1}(\hat{\mathbf{q}}_a) e_{l_2}(\hat{\mathbf{q}}_a) e_{l_3}(\hat{\mathbf{q}}_b) \times e_{l_4}(\hat{\mathbf{q}}_b) P_L(\hat{\mathbf{q}}_a \cdot \hat{\mathbf{q}}_b). \tag{28}$$

Since the Wigner-3j symbol vanishes if $l_1 + l_2 + L = \text{odd}$, this expression can only be used to estimate even terms.

To measure all configurations of the trispectrum is, needless to say, a daunting task. Aside from the computational expense, one must also treat complications associated with estimators of harmonics on a fraction of the sky. Even for an all-sky CMB experiment, the removal of galactic foregrounds will limit the data to a smaller fraction of the sky $f_{\rm sky}$.

B. Signal-to-noise

Returning to the estimator of Eq. (26), one can calculate the Gaussian *noise* variance of the estimator,

$$\langle \hat{T}^{l_1 l_2 *}_{l_3 l_4}(L) \hat{T}^{l_1 l_2}_{l_3 l_4}(L') \rangle = (2L+1) \delta_{LL'} C^{\rm tot}_{l_1} C^{\rm tot}_{l_2} C^{\rm tot}_{l_3} C^{\rm tot}_{l_4}, \tag{29}$$

if no two l's are equal. Here $C^{\rm tot}_l$ is the sum of all contributions to the power spectrum including the intrinsic CMB fluctuations, instrumental noise, and residual foreground contamination.

From the permutation properties of Q (or T) in Eq. (16), the full covariance of the estimators then becomes

$$\frac{\langle \hat{T}^{l_1 l_2 *}_{l_3 l_4}(L) \hat{T}^{l_1' l_2'}_{l_3' l_4'}(L') \rangle}{(2L+1) C^{\rm tot}_{l_1} C^{\rm tot}_{l_2} C^{\rm tot}_{l_3} C^{\rm tot}_{l_4}} = \delta_{LL'} \delta^{12}_{34} + (2L'+1) \Bigg[(-1)^{l_2+l_3} \times \begin{Bmatrix} l_1 & l_2 & L \\ l_4 & l_3 & L' \end{Bmatrix} \delta^{13}_{24} + (-1)^{L+L'} \begin{Bmatrix} l_1 & l_2 & L \\ l_3 & l_4 & L' \end{Bmatrix} \delta^{14}_{32} \Bigg], \tag{30}$$

if no two l's in the primed and unprimed sets are equal. Here

$$\delta^{ab}_{cd} = [\delta_{l_1 l_a} \delta_{l_2 l_b} + (-1)^{\Sigma_U} \delta_{l_1 l_b} \delta_{l_2 l_a}][\delta_{l_3 l_c} \delta_{l_4 l_d} + (-1)^{\Sigma_L} \delta_{l_3 l_d} \delta_{l_4 l_c}] + [a \leftrightarrow c][b \leftrightarrow d] \tag{31}$$

accounts for the permutations within the three fundamental pairings. Recall that $\Sigma_U = l_1 + l_2 + L$ and $\Sigma_L = l_3 + l_4 + L$. The two terms involving the Wigner-6j symbol reflect the fact that alternate pairings of the indices supply redundant information in both the signal and the noise.

If any two l's are equal, then the covariance has extra terms associated with the internal pairings in the primed and unprimed sets. Based on the fundamental relation

$$\langle \hat{T}^{l_1 l_1 *}_{l_3 l_4}(L) \hat{T}^{l_1' l_1'}_{l_3' l_4'}(L') \rangle = (-1)^{l_1 + l_1'} \delta_{L0} \delta_{L'0} \sqrt{(2l_1+1)(2l_1'+1)} [\delta_{l_3 l_3'} \delta_{l_4 l_4'} + (-1)^{\Sigma_L} \delta_{l_3 l_4'} \delta_{l_4 l_3'}] C_{l_1} C_{l_1'} C_{l_3} C_{l_4}, \tag{32}$$

other pairings can be found through the permutation properties of Q (or T). No fundamentally new terms are introduced if three or four l's are equal but each set of possible internal pairings in the primed and unprimed sets must be separately accounted for.

The total signal-to-noise for each L in the four-point spectrum is

$$\left(\frac{S}{N} \right)^2 \equiv \sum_{l_1 l_2 l_3 l_4 L} \sum_{l_1' l_2' l_3' l_4' L'} \langle \hat{T}^{l_1 l_2 *}_{l_3 l_4}(L) \rangle [\text{Cov}^{-1}] \langle \hat{T}^{l_1' l_2'}_{l_3' l_4'}(L') \rangle \approx \sum_L \sum_{l_1 > l_2 > l_3 > l_4} \frac{1}{2L+1} \frac{|\hat{T}^{l_1 l_2}_{l_3 l_4}(L)|^2}{C^{\rm tot}_{l_1} C^{\rm tot}_{l_2} C^{\rm tot}_{l_3} C^{\rm tot}_{l_4}}, \tag{33}$$

where "Cov^{-1}" indicates the matrix inverse, with elements labeled by their configuration (l_1, l_2, l_3, l_4, L), of the covariance in Eq. (30). In the second line, the restricted sum eliminates the $4! = 24$ redundant permutations above and neglects the signal-to-noise contributed when the the l's are equal. In the high signal-to-noise regime, one must also include the sample variance of the signal. On a cut sky, the considerations of Appendix B imply that the overall $(S/N)^2$ is reduced by a factor of $f_{\rm sky}$.

Note that if the sum in Eq. (33) is not restricted the covariance supplied by the alternate pair orderings in Eq. (16) necessarily contains off diagonal terms that mix L and L'. The covariance is distributed across many L's and can lead to overestimates of the signal-to-noise in four-point related statistics by a factor of $\sqrt{3}$.

C. Power spectrum covariance

The trispectrum can affect two-point or power spectrum statistics by introducing a covariance between the estimators. The covariance of power spectrum estimators averaged over m is given by

$$\langle \hat{C}_{l_1}\hat{C}_{l_2}\rangle = \frac{1}{2l_1+1}\frac{1}{2l_2+1}\sum_{m_1m_2}\langle \Theta_{l_1m_1}\Theta^*_{l_1m_1}\Theta_{l_2m_2}\Theta^*_{l_2m_2}\rangle - \langle \hat{C}_{l_1}\rangle\langle \hat{C}_{l_2}\rangle$$

$$= \frac{1}{\sqrt{2l_1+1}}\frac{1}{\sqrt{2l_2+1}}(-1)^{l_1+l_2}Q^{l_1l_1}_{l_2l_2}(0) - \langle \hat{C}_{l_1}\rangle\langle \hat{C}_{l_2}\rangle. \quad (34)$$

The expression for the covariance can be further broken into its Gaussian and non-Gaussian pieces

$$\langle \hat{C}_{l_1}\hat{C}_{l_2}\rangle = \frac{2}{2l_1+1}C^2_{l_1}\delta_{l_1l_2} + \frac{(-1)^{l_1+l_2}}{\sqrt{(2l_1+1)(2l_2+1)}} \times \left[\mathcal{T}^{l_1l_1}_{l_2l_2}(0) + \frac{2}{\sqrt{(2l_1+1)(2l_2+1)}} \times \sum_{L=|l_1-l_2|}^{l_1+l_2}(-1)^L \mathcal{T}^{l_1l_2}_{l_1l_2}(L)\right], \quad (35)$$

where recall that $\mathcal{T}$ is the reduced trispectrum of Eq. (23). The effect of covariance for the signal-to-noise for the estimation of a set of underlying cosmological parameters p_i can be calculated through the Fisher matrix

$$F_{ij} = \sum_{l_1l_2}\frac{\partial C_{l_1}}{\partial p_i}[\mathrm{Cov}^{-1}]\frac{\partial C_{l_2}}{\partial p_j}, \quad (36)$$

where "Cov^{-1}" indicates the matrix inverse of the covariance in Eq. (35). In particular, if the only parameter of interest is the overall amplitude A of a known template shape, then $F_{AA}=(S/N)^2$ (see Ref. [3]).

IV. POWER SPECTRA OF QUADRATIC STATISTICS

Measuring all of the configurations of the trispectrum or four-point function is a daunting challenge. In this section we consider statistics based on the identification of points in pairs in the four-point function. These quadratic statistics may be optimized in signal-to-noise for their power spectra by filtering the original temperature field. We begin with general definitions for the quadratic fields in harmonic space (Sec. II A) and continue through a discussion of filters (Sec. IV B) to a consideration of specific quadratic statistics (Sec. IV C–IV H) and related cubic statistics (Sec. IV I). The specific statistic and filter set that optimizes the signal-to-noise will depend on the configuration dependence of the trispectrum signal that is to be extracted.

A. General definitions

To probe various aspects of the trispectrum, we can form the two-point or power spectrum statistics of a quadratic combination of the underlying field. To enhance the signal-to-noise, we begin by filtering the fields before collapsing the configuration,

$$\Theta^a(\hat{\mathbf{n}}) = \sum_{lm}\Theta_{lm}f^a_l Y^m_l(\hat{\mathbf{n}}), \quad (37)$$

where the index $a=1,4$ to allow for four independent filters on the fields. In general, the identification of points in pairs implies that each pair (ab) involves a quadratic combination of the filtered field which in turn involves a mode coupling sum of the harmonic coefficients

$$x^{ab}_{LM} = (-1)^M\sum_{l_1m_1}\sum_{l_2m_2}x^{ab}_{l_1l_2}(L)\Theta_{l_1m_1}\Theta_{l_2m_2} \times \sqrt{\frac{2L+1}{4\pi}}\begin{pmatrix} l_1 & l_2 & L \\ m_1 & m_2 & -M\end{pmatrix}, \quad (38)$$

where

$$x^{ab}_{l_1l_2}(L) = f^a_{l_1}f^b_{l_2}\sqrt{(2l_1+1)(2l_2+1)}x_{l_1l_2}(L), \quad (39)$$

and $x_{l_1l_2}(L)$ represents different weights for different statistics x as specified below. The power spectra statistics relating two general quadratic statistics x and $\tilde{x}$ may be separated into the non-Gaussian signal and Gaussian noise as

$$\langle x^{12*}_{LM}\tilde{x}^{34}_{L'M'}\rangle = \delta_{LL'}\delta_{MM'}(C^{x\tilde{x}}_L + N^{x\tilde{x}}_L), \quad (40)$$

where

$$C^{x\tilde{x}}_L = \frac{1}{4\pi}\frac{1}{2L+1}\sum_{l_1l_2l_3l_4}x^{12*}_{l_1l_2}(L)\tilde{x}^{34}_{l_3l_4}(L)T^{l_1l_2}_{l_3l_4}(L), \quad (41)$$

and the Gaussian noise is

$$N^{x\tilde{x}}_L = \frac{1}{4\pi}\sum_{l_1l_2}x^{12*}_{l_1l_2}(L)[\tilde{x}^{34}_{l_1l_2}(L)+\tilde{x}^{34}_{l_2l_1}(L)]C^{\mathrm{tot}}_{l_1}C^{\mathrm{tot}}_{l_2}. \quad (42)$$

It will be useful in the following discussion of noise variance to also define the following two auxiliary power spectra:

$$V^{x\tilde{x}(12)}_L = \frac{1}{4\pi}\sum_{l_1l_2}x^{12*}_{l_1l_2}(L)[\tilde{x}^{12}_{l_1l_2}(L)+\tilde{x}^{12}_{l_2l_1}(L)]C^{\mathrm{tot}}_{l_1}C^{\mathrm{tot}}_{l_2},$$

$$V_L^{x\tilde{x}(34)} \frac{1}{4\pi} \sum_{l_1 l_2} x_{l_1 l_2}^{34 *}(L)[\tilde{x}_{l_1 l_2}^{34}(L) + \tilde{x}_{l_2 l_1}^{34}(L)] C_{l_1}^{\rm tot} C_{l_2}^{\rm tot}. \tag{43}$$

The signal-to-noise ratio in this power spectrum statistic can be calculated from Eq. (30) for the covariance of the trispectrum,

$$\langle \hat{C}_L^{x\tilde{x}} \hat{C}_L^{x'\tilde{x}'} \rangle \approx \frac{1}{2L+1} [\langle V_L^{xx'(12)} \rangle \langle V_L^{\tilde{x}\tilde{x}'(34)} \rangle + \langle N_L^{x\tilde{x}'} \rangle \langle N_L^{\tilde{x}x'} \rangle], \tag{44}$$

such that

$$\left(\frac{S}{N} \right)^2 \approx \sum_{L x \tilde{x} x' \tilde{x}'} \frac{\langle C_L^{x\tilde{x}} \rangle \langle C_L^{x'\tilde{x}'} \rangle}{\langle \hat{C}_L^{x\tilde{x}} \hat{C}_L^{x'\tilde{x}'} \rangle}. \tag{45}$$

Strictly speaking, this is an inequality since we have neglected the covariance between L's dictated by the trispectrum covariance, Eq. (30). Since the trispectrum covariance is distributed broadly in the allowed L's, this signal-to-noise estimate is reasonable if we restrict the range of interest in L to a small fraction of the allowed range. The covariance can at most reduce the total signal-to-noise by a factor of $\sqrt{3}$ for the three unique pairings in the trispectrum.

B. Filters

The filters and specific form of the statistic x can be chosen to eliminate Gaussian noise bias and/or maximize the signal-to-noise. If (f_l^1, f_l^2) and (f_l^3, f_l^4) do not overlap in l, then the Gaussian noise bias of Eq. (42) vanishes. Furthermore, trispectrum covariance between differing L's is identically zero and Eq. (45) becomes a strict equality.

For example the two filters may be band limited in mutually exclusive bands or parity limited,

$$\Theta_e(\hat{\mathbf{n}}) \equiv \frac{1}{2}[\Theta(\hat{\mathbf{n}}) + \Theta(-\hat{\mathbf{n}})],$$

$$f_l^1 = f_l^2 \equiv \begin{cases} 1, & l = \text{even}, \\ 0, & l = \text{odd}, \end{cases} \tag{46}$$

$$\Theta_o(\hat{\mathbf{n}}) \equiv \frac{1}{2}[\Theta(\hat{\mathbf{n}}) - \Theta(-\hat{\mathbf{n}})],$$

$$f_l^3 = f_l^4 \equiv \begin{cases} 0, & l = \text{even}, \\ l, & l = \text{odd}. \end{cases} \tag{47}$$

This choice does not eliminate the auxiliary variance power spectra in Eq. (43) and more generally does not maximize the total signal-to-noise. Only if the filters are equal in pairs $f_l^1 = f_l^3$ and $f_l^2 = f_l^4$ are the noise and auxiliary variance power spectra equal such that

$$\langle \hat{C}_L^{x\tilde{x}} \hat{C}_L^{x'\tilde{x}'} \rangle \approx \frac{1}{2L+1} (\langle N_L^{xx'} \rangle \langle N_L^{\tilde{x}\tilde{x}'} \rangle + \langle N_L^{x\tilde{x}'} \rangle \langle N_L^{\tilde{x}x'} \rangle), \tag{48}$$

becomes the familiar form for the variance of the power spectra of a set of Gaussian random fields x.

A comparison of the signal-to-noise in the full trispectrum, Eq. (33) and in a particular quadratic statistic x Eq. (45), shows that the latter approaches the former if

$$x_{l_1 l_2}^{12}(L) x_{l_3 l_4}^{34}(L) \to w(L) \frac{T_{l_3 l_4}^{l_1 l_2}(L)}{C_{l_1}^{\rm tot} C_{l_2}^{\rm tot} C_{l_3}^{\rm tot} C_{l_4}^{\rm tot}}, \tag{49}$$

where $w(L)$ is an arbitrary function of L. To the extent that the right-hand side is factorable in l_a, $a = 1,4$ the filter functions f_l^a can be chosen to construct this optimal statistic. Since the trispectrum is in general not factorable, we will next consider a wide range of choices for the quadratic x statistic which can be used to construct optimal statistics for various types of trispectrum signals.

C. Temperature-temperature

The simplest quadratic statistic that we can form is the product of the filtered temperature field itself,

$$\Theta^a(\hat{\mathbf{n}}) \Theta^b(\hat{\mathbf{n}}) \equiv s^{ab}(\hat{\mathbf{n}}) = \sum_{LM} s_{LM}^{ab} Y_L^M(\hat{\mathbf{n}}), \tag{50}$$

where s_{LM}^{ab} is given by the general prescription of Eq. (38) with $x = s$ and the weighting

$$s_{l_1 l_2}(L) = \begin{pmatrix} l_1 & l_2 & L \\ 0 & 0 & 0 \end{pmatrix} \quad \text{even}. \tag{51}$$

"Even" denotes the fact that s selects out $l_1 + l_2 + L = \text{even}$ by virtue of the Wigner-3j symbol. The non-Gaussian power spectrum C_L^{ss} is then given by Eq. (41) in terms of the trispectrum. The total signal-to-noise of this statistic can be estimated by retaining just the $x = x' = \tilde{x} = \tilde{x}' = s$ terms in Eq. (45).

D. Temperature-gradient

The product of the filtered temperature field and the gradient of the filtered temperature field probes another aspect the trispectrum. This product is a vector field on the sky and may be broken up into components as

$$\Theta^a(\hat{\mathbf{n}}) \nabla_i \Theta^b(\hat{\mathbf{n}}) \equiv \sum_{\pm} \frac{1}{\sqrt{2}} [\alpha_1 \pm i \alpha_2]^{ab}(\hat{\mathbf{n}}) \frac{1}{\sqrt{2}} (\hat{\mathbf{e}}_\phi \mp \hat{\mathbf{e}}_\theta)_i. \tag{52}$$

The components $\alpha_1 \pm i \alpha_2$ are spin-1 objects that can be decomposed in the spin-1 spherical harmonics [9],

$$[\alpha_1 \pm i \alpha_2]^{ab}(\hat{\mathbf{n}}) = \sum_{LM} (c \pm i g)_{LM}^{ab} \, {}_{\pm 1}Y_L^M(\hat{\mathbf{n}}), \tag{53}$$

where c and g are the multipole analogues of the curl and gradient pieces. These quadratic statistics again follow the general form of Eq. (38) with $x = c, g$ and weightings

$$c_{l_1 l_2}(L) \equiv -\sqrt{l_2(l_2+1)} \begin{pmatrix} l_1 & l_2 & L \\ 0 & -1 & 1 \end{pmatrix} \quad \text{odd} \tag{54}$$

$$g_{l_1 l_2}(L) \equiv i\sqrt{l_2(l_2+1)} \begin{pmatrix} l_1 & l_2 & L \\ 0 & -1 & 1 \end{pmatrix} \quad \text{even}. \tag{55}$$

Here and below "even" ("odd") denotes the fact that the expression holds for $l_1+l_2+L=$even (odd) and vanishes otherwise. If the trispectrum is parity invariant (zero if $l_1+l_2+l_3+l_4=$odd), the cross power spectra $C_L^{gc}=0=C_L^{sc}$ vanish. The remaining power spectra and their covariance are described by the general forms of Eqs. (41), (42), and (44).

E. Gradient-gradient

The product of temperature gradients can in general be decomposed into three quadratic statistics,

$$[\nabla_i \Theta_a(\hat{\mathbf{n}})][\nabla_j \Theta_b(\hat{\mathbf{n}})] \equiv t^{ab}(\hat{\mathbf{n}}) g_{ij}(\hat{\mathbf{n}}) + \sum_{\pm} [q \pm iu]^{ab}(\hat{\mathbf{n}}) \times \sigma_{ij}^{\pm}(\hat{\mathbf{n}}) + v(\hat{\mathbf{n}}) \epsilon_{ij}(\hat{\mathbf{n}}), \tag{56}$$

where g_{ij} is the metric on the two-sphere,

$$\sigma_{ij}^{\pm}(\hat{\mathbf{n}}) = \frac{1}{2}(\hat{\mathbf{e}}_\theta \mp \hat{\mathbf{e}}_\phi)_i (\hat{\mathbf{e}}_\theta \mp \hat{\mathbf{e}}_\phi)_j, \tag{57}$$

gives the basis for a trace-free symmetric tensor field on the sky, and

$$\epsilon_{ij}(\hat{\mathbf{n}}) = (\mathbf{e}_\theta)_j (\mathbf{e}_\phi)_i - (\mathbf{e}_\theta)_i (\mathbf{e}_\phi)_j \tag{58}$$

gives the basis for a trace-free antisymmetric tensor field on the sky. The flat-sky versions of these statistics were first employed in Ref. [10] for CMB lensing and note that q, u, v are analogous to the similarly named Stokes parameters for polarization.

As is the case for the CMB polarization, these three fields may be decomposed into multipole moments of the spherical harmonics and spin-2 spherical harmonics [9],

$$t^{ab}(\hat{\mathbf{n}}) = \sum_{LM} t_{LM}^{ab} Y_L^M(\hat{\mathbf{n}}),$$

$$v^{ab}(\hat{\mathbf{n}}) = \sum_{LM} v_{LM}^{ab} Y_L^M(\hat{\mathbf{n}}),$$

$$[q \pm iu]^{ab}(\hat{\mathbf{n}}) = \sum_{LM} (e \pm ib)_{LM\ \pm 2}^{ab} Y_L^M(\hat{\mathbf{n}}), \tag{59}$$

where the moments follow the general prescription of Eq. (38) with $x=t,e,b,v$ and weights

$$t_{l_1 l_2}(L) \equiv -\frac{1}{2}\sqrt{l_1(l_1+1)}\sqrt{l_2(l_2+1)} \begin{pmatrix} l_1 & l_2 & L \\ -1 & 1 & 0 \end{pmatrix} \quad \text{even},$$

$$v_{l_1 l_2}(L) \equiv \frac{i}{2}\sqrt{l_1(l_1+1)}\sqrt{l_2(l_2+1)} \begin{pmatrix} l_1 & l_2 & L \\ -1 & 1 & 0 \end{pmatrix} \quad \text{odd},$$

$$e_{l_1 l_2}(L) \equiv \frac{1}{2}\sqrt{l_1(l_1+1)}\sqrt{l_2(l_2+1)} \begin{pmatrix} l_1 & l_2 & L \\ -1 & -1 & 2 \end{pmatrix} \quad \text{even},$$

$$b_{l_1 l_2}(L) \equiv -\frac{i}{2}\sqrt{l_1(l_1+1)}\sqrt{l_2(l_2+1)} \times \begin{pmatrix} l_1 & l_2 & L \\ -1 & -1 & 2 \end{pmatrix} \quad \text{odd}. \tag{60}$$

If the trispectrum is parity invariant, cross power spectra exist only among (t,e,g,s) and (β,v,c). These power spectra and their covariance again are described by the general forms of Eqs. (41), (42), and (44).

F. Temperature-Hessian

Similarly to the gradient-gradient case, the product of the temperature and the second derivatives or Hessian of the temperature field can be decomposed into three quadratic statistics,

$$\Theta^a(\hat{\mathbf{n}}) \nabla_i \nabla_j \Theta^b(\hat{\mathbf{n}}) \equiv h^{ab}(\hat{\mathbf{n}}) g_{ij}(\hat{\mathbf{n}}) + \sum_{\pm} [\eta_1 \pm i\eta_2]^{ab}(\hat{\mathbf{n}}) \sigma_{ij}^{\pm}(\hat{\mathbf{n}}), \tag{61}$$

which themselves may be decomposed into multipole moments of the spherical harmonics and spin-2 spherical harmonics,

$$h^{ab}(\hat{\mathbf{n}}) = \sum_{LM} h_{LM}^{ab} Y_L^M(\hat{\mathbf{n}}),$$

$$[\eta_1 \pm i\eta_2]^{ab}(\hat{\mathbf{n}}) = \sum_{LM} (\epsilon \pm i\beta)_{LM\ \pm 2}^{ab} Y_L^M(\hat{\mathbf{n}}), \tag{62}$$

where the moments follow the general prescription of Eq. (38) with $x=h,\epsilon,\beta$ and weights

$$h_{l_1 l_2}(L) \equiv -\frac{1}{2} l_2(l_2+1) \begin{pmatrix} l_1 & l_2 & L \\ 0 & 0 & 0 \end{pmatrix} \quad \text{even},$$

$$= -\frac{1}{2} l_2(l_2+1) s_{l_1 l_2},$$

$$\epsilon_{l_1 l_2}(L) \equiv \frac{1}{2}\sqrt{\frac{(l_2+2)!}{(l_2-2)!}} \begin{pmatrix} l_1 & l_2 & L \\ 0 & -2 & 2 \end{pmatrix} \quad \text{even},$$

$$\beta_{l_1 l_2}(L) \equiv -\frac{i}{2}\sqrt{\frac{(l_2+2)!}{(l_2-2)!}} \begin{pmatrix} l_1 & l_2 & L \\ 0 & -2 & 2 \end{pmatrix} \quad \text{odd}. \tag{63}$$

Again parity invariance requires that power spectra exist only between (h,ϵ,t,e,s) and (β,b,v,c). Likewise the general formula for power spectra and their covariance again apply.

G. Temperature-temperature Hessian

Auxiliary two-point statistics can be formed from the fundamental ones above. For example

$$\nabla_i\nabla_j[\Theta^a(\hat{\mathbf{n}})\Theta^b(\hat{\mathbf{n}})]\equiv\tilde{t}^{ab}(\hat{\mathbf{n}})g_{ij}(\hat{\mathbf{n}}) + \sum_{\pm}[\tilde{q}\pm i\tilde{u}]^{ab}(\hat{\mathbf{n}})\sigma^{\pm}_{ij}(\hat{\mathbf{n}}), \tag{64}$$

and

$$\tilde{t}^{ab}(\hat{\mathbf{n}})=\sum_{LM}\tilde{t}^{ab}_{LM}Y^M_L(\hat{\mathbf{n}}),$$

$$[\tilde{q}+i\tilde{u}]^{ab}(\hat{\mathbf{n}})=\sum_{LM}(\tilde{e}+i\tilde{b})^{ab}_{LM\ \pm 2}Y^M_L(\hat{\mathbf{n}}) \tag{65}$$

imply that

$$\tilde{t}_{l_1l_2}=t_{l_1l_2}+t_{l_2l_1}+h_{l_1l_2}+h_{l_2l_1}=-\frac{L(L+1)}{2}\begin{pmatrix} l_1 & l_2 & L\\ 0 & 0 & 0\end{pmatrix},$$

$$\tilde{e}_{l_1l_2}=e_{l_1l_2}+e_{l_2l_1}+\epsilon_{l_1l_2}+\epsilon_{l_2l_1} =\frac{1}{2}\sqrt{\frac{(L+2)!}{(L-2)!}}\begin{pmatrix} l_1 & l_2 & L\\ 0 & 0 & 0\end{pmatrix},$$

$$\tilde{b}_{l_1l_2}=b_{l_1l_2}+b_{l_2l_1}+\beta_{l_1l_2}+\beta_{l_2l_1}=0.$$

Again power spectra follow from the general relations.

H. Temperature-gradient divergence

The divergence of the temperature-gradient field of Sec. IV D is also an auxiliary statistic

$$\nabla^i[\Theta^a(\hat{\mathbf{n}})\nabla_i\Theta^b(\hat{\mathbf{n}})]\equiv d^{ab}(\hat{\mathbf{n}})Y^M_L(\hat{\mathbf{n}}), \tag{66}$$

with

$$d^{ab}(\hat{\mathbf{n}})=\sum_{LM}d^{ab}_{LM}Y^M_L(\hat{\mathbf{n}}). \tag{67}$$

The weights are related to the others as

$$d_{l_1l_2}=\sqrt{L(L+1)l_2(l_2+1)}\begin{pmatrix} l_1 & l_2 & L\\ 0 & -1 & 1\end{pmatrix}\ \text{even},$$

$$=-i\sqrt{L(L+1)}g_{l_1l_2}=2t_{l_1l_2}+2h_{l_1l_2}. \tag{68}$$

Again power spectra follow from the general relations.

I. Cubic statistics

Finally the cross correlation of cubic statistics with linear statistics are also related to the quadratic statistics introduced above. For example

$$\langle\Theta^1(\hat{\mathbf{n}}_1)\Theta^2(\hat{\mathbf{n}}_1)\Theta^3(\hat{\mathbf{n}}_1)\,\Theta^4(\hat{\mathbf{n}}_2)\rangle =\sum_{lm}(-1)^m[C_l^{ss(3)}+N_l^{ss(3)}]Y_l^{-m}(\hat{\mathbf{n}}_1)Y_l^m(\hat{\mathbf{n}}_2)\,. \tag{69}$$

More generally, the cubic power spectra corresponding to the various x statistics are given by

$$C_l^{x\tilde{x}(3)}=\sum_{l_1l_2l_3L}\frac{1}{4\pi}\frac{1}{2L+1}x^{12*}_{l_1l_2}(L)\tilde{x}^{34}_{l_3l}(L)T^{l_1l_2}_{l_3l}(L), \tag{70}$$

with Gaussian noise bias

$$N_l^{x\tilde{x}(3)}=\frac{1}{4\pi}\sum_{l_1L}x^{12*}_{l_1l_2}(L)[\tilde{x}^{34}_{l_1l}(L)+\tilde{x}^{34}_{ll_1}(L)]C^{\rm tot}_{l_1}C^{\rm tot}_l, \tag{71}$$

and auxiliary noise variance

$$V_l^{x\tilde{x}(3,12)}=\frac{1}{4\pi}\sum_{l_1L}x^{12*}_{l_1l_2}(L)[\tilde{x}^{12}_{l_1l}(L)+\tilde{x}^{12}_{ll_1}(L)]C^{\rm tot}_{l_1}C^{\rm tot}_l,$$

$$V_l^{x\tilde{x}(3,34)}=\frac{1}{4\pi}\sum_{l_1L}x^{34*}_{l_1l_2}(L)[\tilde{x}^{34}_{l_1l}(L)+\tilde{x}^{34}_{ll_1}(L)]C^{\rm tot}_{l_1}C^{\rm tot}_l, \tag{72}$$

i.e., the multipole index of the power spectra is no longer the diagonal of the trispectrum configuration but rather one of its sides. These cubic statistics thus probe a different projection of the trispectrum information but are based on the same set of filters and employ the same statistical formalism.

V. CMB LENSING

In this section, we consider the trispectrum signal generated by the weak gravitational lensing of the CMB temperature anisotropies by the large-scale structure in the Universe. In Sec. V A we derive the full trispectrum for lensing and relate it to the underlying deflection (or convergence) power spectrum. Zaldarriaga [6] previously considered the lensing trispectrum in the small-scale or flat-sky approximation. The gravitational lensing effect is known to be dominated by potential fluctuations on the largest scales where an all-sky treatment of the trispectrum is desirable [7]. In Sec. V B, we show that the signal-to-noise in the trispectrum is both large and highly configuration dependent for experiments that can resolve multipole moments $l\gtrsim 1000$. The divergence statistic introduced in Sec. IV H is shown in Sec. V C to be optimal for measuring the underlying deflection power spectrum at its peak at low multipoles. It benefits from substantially higher signal-to-noise as compared with the gradient-gradient quadratic statistics introduced by Zaldarriaga and Seljak [10]. Finally we consider tests for the robustness of

the divergence statistic with differing filter sets in Sec. V D and the degradation in power spectrum estimation from lensing covariance in Sec. V E.

A. General trispectrum

We begin by briefly reviewing the effect of gravitational lensing on the harmonics of the CMB temperature field and refer the reader to Ref. [7] for details of its calculation in a given cosmology. For reference, we employ the same cold dark matter model with a cosmological constant (ΛCDM) used there, with parameters $\Omega_m=0.35$, $\Omega_\Lambda=0.65$, $h=0.65$, $n=1$, and $\delta_H=4.2\times10^{-5}$.

Weak lensing of the CMB remaps the primary anisotropy according to the deflection angle $\nabla\phi(\hat{\mathbf{n}})$,

$$\Theta(\hat{\mathbf{n}})=\tilde{\Theta}(\hat{\mathbf{n}}+\nabla\phi)$$
$$=\tilde{\Theta}(\hat{\mathbf{n}})+\nabla_i\phi(\hat{\mathbf{n}})\nabla^i\tilde{\Theta}(\hat{\mathbf{n}})+\cdots, \tag{73}$$

where the tilde represents the unlensed field and $\cdots$ represents higher order terms in the Taylor expansion. The lensing potential field $\phi(\hat{\mathbf{n}})$ is a lensing-probability weighted projection of the Newtonian potential along the line of sight [see Ref. [7], Eq. (21)].

The spherical harmonic coefficients of the lensed CMB temperature field become

$$\Theta_{lm}\approx\tilde{\Theta}_{lm}+\int d\hat{\mathbf{n}}Y_l^{m*}(\hat{\mathbf{n}})\nabla_i\phi(\hat{\mathbf{n}})\nabla^i\tilde{\Theta}(\hat{\mathbf{n}})+\cdots$$
$$=\tilde{\Theta}_{lm}+\sum_{LM}\sum_{l'm'}\phi_{LM}\tilde{\Theta}_{l'm'}(-1)^m$$
$$\times\begin{pmatrix} l & l' & L \\ m & -m' & -M\end{pmatrix}F_{lLl'}+\cdots, \tag{74}$$

where

$$\sqrt{\frac{4\pi}{(2l+1)(2l'+1)(2L+1)}}F_{lLl'}=\frac{1}{2}[L(L+1)+l'(l'+1)-l(l+1)]\begin{pmatrix} l & l' & L \\ 0 & 0 & 0\end{pmatrix},$$
$$=-\sqrt{L(L+1)l'(l'+1)}\begin{pmatrix} l & l' & L \\ 0 & -1 & 1\end{pmatrix}\quad\text{even}, \tag{75}$$

where recall that ''even'' denotes the fact that only $l+l'+L=$even is nonvanishing. Gravitational lensing generates a change in the power spectrum that has been well studied [11–13,7]. It produces two changes to the four-point function. The first is that the unlensed $\tilde{C}_l$ in the Gaussian four-point contribution must be replaced with the lensed C_l. The second is that it generates a trispectrum with an underlying reduced form [see Eq. (23)] of

$$\mathcal{T}^{l_1l_2}_{l_3l_4}(L)=C_L^{\phi\phi}\tilde{C}_{l_2}\tilde{C}_{l_4}F_{l_1Ll_2}F_{l_3Ll_4}. \tag{76}$$

Note the geometric interpretation: the lensing generates a trispectrum or quadrilateral configuration of $l_1\cdots l_4$ where one of the diagonals is supported by the lensing potential power spectrum $C_L^{\phi\phi}$. Note that the power spectrum of the deflection field is given by $L(L+1)C_L^{\phi\phi}$ and is the fundamental quantity of interest. It is plotted in Fig. 1 for the fiducial ΛCDM model. It is important to note that most of the power in the deflections is coming from a rather large scale or low multipole $L\approx50$. We contrast this with the more familiar convergence power spectrum $C_L^{\kappa\kappa}=[L(L+1)/2]^2C_L^{\phi\phi}$ which peaks at much smaller angular scales.

B. Total signal-to-noise

From the considerations of Sec. III B, we can calculate the total signal-to-noise in the trispectrum for lensing in the full-sky formalism. Flat-sky estimates of the total signal-to-noise have been calculated in Ref. [6] (see also Appendix B). The all-sky expressions are cumbersome to calculate due to the presence of the Wigner-6j symbol that expresses the alternate recouplings of the trispectrum l's. We use the recursion technique outlined in Appendix A for these calculations.

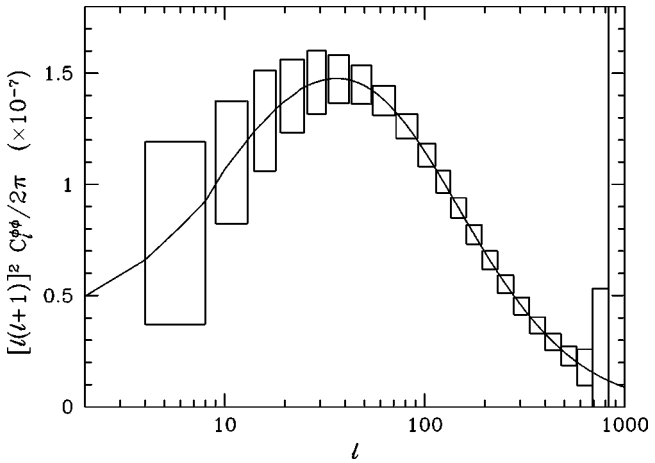

FIG. 1. The power spectrum of the deflection angle in the fiducial ΛCDM model. Error boxes represent the 1σ errors from Gaussian noise on the divergence statistic binned in the bands shown. The divergence estimator of Eqs. (80) and (81) is optimal for the low multipoles and reduces the variance in the power spectrum estimation by more than an order of magnitude as compared with the gradient-gradient statistics of Ref. [10].

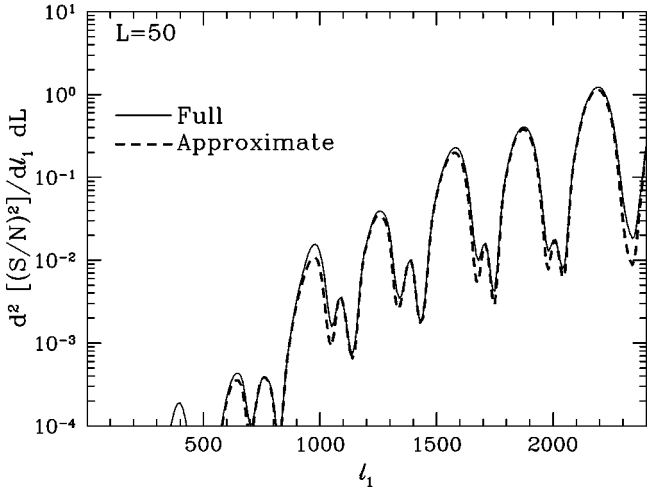

FIG. 2. Contributions to the $(S/N)^2$ from trispectra configurations with a fixed diagonal L and maximum side length l_1, summed over the remaining three sides. Solid lines represent the full calculation of the trispectrum terms; dashed lines represent the pairwise approximation of Eq. (77). The signal-to-noise in the low, L trispectrum is highly dependent on the configuration.

In Fig. 2, we show the signal-to-noise contributions in a given mode $L=50$ of the trispectrum from a given l_1 (summed over l_2,l_3,l_4) assuming an ideal experiment $C_l^{\rm tot}=C_l$. The signal-to-noise is quite high and approaches unity per l_1 mode and L mode at $l_1\approx 2000$. Moreover, the contributions as a function of l_1 show striking features. These features can be understood by approximating the trispectrum by its fundamental pairing $(l_1,l_2),(l_3,l_4)$ in Eq. (23),

$$T^{l_1l_2}_{l_3l_4}(L)\approx P^{l_1l_2}_{l_3l_4}=C_L^{\phi\phi}(\tilde{C}_{l_2}F_{l_1Ll_2}+\tilde{C}_{l_1}F_{l_2Ll_1})(\tilde{C}_{l_4}F_{l_3Ll_4}+\tilde{C}_{l_3}F_{l_4Ll_3}). \quad (77)$$

Figure 2 (dashed lines) verifies that this is a very good approximation for the range of interest $l_1\gg L$. The reason is that these configurations represent flattened quadrilaterals where one diagonal is much greater than the other. Since lensing effects peak at low L, the other pairings are correspondingly suppressed. These properties are hidden in the real-space four-point function and highlight the benefit of considering harmonic-space statistics.

To the extent that $\tilde{C}_l$ is constant, the two terms within each set of parentheses in Eq. (77) cancel. Thus, the trispectrum picks out features in the underlying unlensed power spectrum, specifically those due to the acoustic peaks in the power spectrum. Note that the effects on the power spectrum itself exhibit the same effect: lensing acts to smooth the acoustic features in the spectrum. This structure implies that optimizing the l range of filters in the quadratic statistics is important for maximizing the signal-to-noise.

The cumulative signal-to-noise integrating out to $l_1=l_{\rm max}$ as a function of L in an ideal experiment is shown in Fig. 3. The approximation of Eq. (77) begins to break down as L approaches $l_{\rm max}$ but always in the sense that it *underestimates* the total signal-to-noise (dashed lines vs points). This

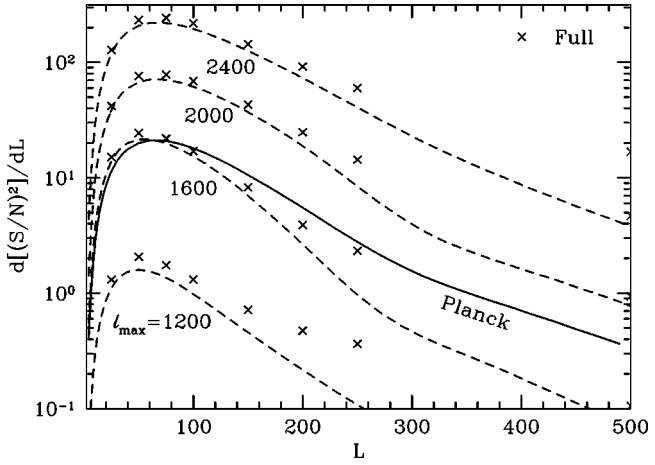

FIG. 3. Cumulative signal-to-noise in the trispectra configurations with the diagonal L summed over $l_1\cdots l_4$. Dashed lines represent an ideal experiment where $C_l=C_l^{\rm tot}$ out to a maximum $l=l_{\rm max}$; solid lines represent the Planck experiment. Lines represent the approximation of Eq. (77); points represent the calculation using the full trispectrum for an ideal experiment.

breakdown occurs since the two diagonals of a trispectrum quadrilateral become comparable and either can be supported by the lensing power in Eq. (76). We also show in Fig. 3 (solid lines) the cumulative signal-to-noise for the Planck satellite [14] with $C_l^{\rm tot}$ taken from Ref. [3]. Planck approximates an ideal experiment with $l_{\rm max}\approx 1600$.

Finally, under the approximation of Eq. (77) which slightly underestimates the total signal-to-noise, we can plot the cumulative signal-to-noise summed over all L as a function of $l_{\rm max}$ (see Fig. 4). Again an $l_{\rm max}\approx 1600$ approximates the Planck experiment whose total $(S/N)^2\approx 3100$.

C. Divergence statistic

The structure in the signal-to-noise curves implies that it is important to select a quadratic statistic that captures this

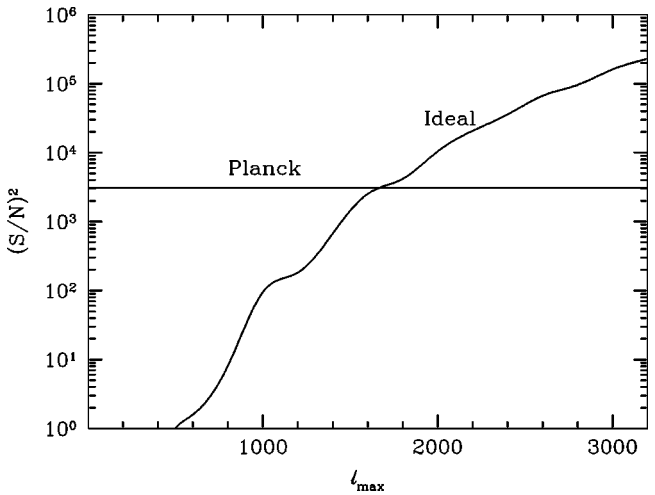

FIG. 4. Approximate total $(S/N)^2$ in the trispectrum for an ideal experiment out to $l=l_{\rm max}$ and the Planck experiment. The Planck experiment approximates an ideal experiment of $l\approx 1600$ with a $(S/N)^2\sim 3100$.

structure. Following the considerations of Sec. IV A, we can search for the quadratic statistic that optimizes the signal-to-noise ratio in the power spectrum of the deflection. Recall that in general the multipole moments of the quadratic statistic with filters f_l^a and f_l^b,

$$x_{LM}^{ab}=(-1)^M\sum_{l_1m_1}\sum_{l_2m_2}x_{l_1l_2}^{ab}(L)\Theta_{l_1m_1}\Theta_{l_2m_2}\times\sqrt{\frac{2L+1}{4\pi}}\begin{pmatrix} l_1 & l_2 & L\\ m_1 & m_2 & -M\end{pmatrix}, \tag{78}$$

are defined in terms of the weight function $x_{l_1l_2}^{ab}$. Under the approximation for the trispectrum of Eq. (77), Eq. (49) gives the optimal weights as

$$x_{l_1l_2}^{12}\propto\frac{\tilde{C}_{l_2}F_{l_1Ll_2}+\tilde{C}_{l_1}F_{l_2Ll_1}}{C_{l_1}^{\rm tot}C_{l_2}^{\rm tot}}. \tag{79}$$

Since the lensing trispectrum is symmetric in $l_1\leftrightarrow l_2$, the temperature-gradient divergence statistic whose weights are

$$x_{l_1l_2}^{12}=\frac{1}{2}(d_{l_1l_2}^{12}+d_{l_2l_1}^{12}),$$

$$d_{l_1l_2}^{12}=f_{l_1}^1f_{l_2}^2F_{l_1Ll_2}\sqrt{\frac{4\pi}{2L+1}} \tag{80}$$

is optimal if the underlying temperature field is first filtered with

$$f_l^1=f_l^3=-\frac{A}{C_l^{\rm tot}},$$

$$f_l^2=f_l^4=\frac{\tilde{C}_l}{C_l^{\rm tot}}. \tag{81}$$

We choose the proportionality constant to return the properly normalized deflection power spectrum

$$A=\sqrt{L(L+1)}(2L+1)\left[\sum_{l_1l_2}\frac{(\tilde{C}_{l_2}F_{l_1Ll_2}+\tilde{C}_{l_1}F_{l_2Ll_1})^2}{2C_{l_1}^{\rm tot}C_{l_2}^{\rm tot}}\right]^{-1}. \tag{82}$$

The signal-to-noise in this statistic is maximal under the assumption that the trispectrum can be approximated as Eq. (77) as is the case for $L\lesssim$several hundred. The total signal-to-noise as calculated from Eq. (45) for Planck is formally $(S/N)^2\approx4050$. Compare this with the gradient-gradient statistic of Ref. [10]; for the unfiltered $e^{ab}(\hat{\mathbf{n}})\equiv\mathcal{E}(\hat{\mathbf{n}})$ the $(S/N)^2\approx135$.

The total signal-to-noise is allowed to exceed the maximum estimate of the previous section since the latter is strictly a lower limit. However the underlying approximation that the estimates at all L's are independent breaks down when integrating over a wide range in L causing a small reduction in the number of independent modes (see Sec. IV A).

The divergence statistic may also be used as a direct estimator of the deflection (or equivalently the convergence) field itself. Generalizing the argument of Ref. [10], one can think of the quadratic statistic x in Eq. (78) as averaging over many independent (high-l or small-scale) realizations of the unlensed CMB field with a fixed realization of the large-scale deflection field

$$\langle x_{LM}^{ab}\rangle_{\rm CMB}=\phi_{LM}\sqrt{\frac{1}{4\pi(2L+1)}}\sum_{l_1l_2}x_{l_1l_2}^{ab}(\tilde{C}_{l_1}F_{l_2Ll_1}+\tilde{C}_{l_2}F_{l_1Ll_2})\quad(L>0). \tag{83}$$

For the divergence statistic filtered as in Eq. (81) all contributions add coherently so that,

$$\langle d_{LM}^{ab}\rangle_{\rm CMB}=\frac{\phi_{LM}}{(2L+1)}\sum_{l_1l_2}\frac{A}{2C_l^{\rm tot}C_l^{\rm tot}}(\tilde{C}_{l_1}F_{l_2Ll_1}+\tilde{C}_{l_2}F_{l_1Ll_2})^2=\sqrt{L(L+1)}\,\phi_{LM}. \tag{84}$$

From the multipole moments one can reconstruct the deflection or convergence map [15]. Of course the fact that we average over only a finite number of independent modes of the primary anisotropy means that the resulting map will be noisy, with noise properties given by the Gaussian noise power spectra.

D. Robustness tests

The divergence statistic contains enough signal-to-noise for Planck that the data may be further subdivided to check for robustness of the statistic. Especially worrisome is the possibility that galactic and extragalactic foregrounds and systematic effects might generate a false signal. Even if these contaminants contribute only Gaussian noise, one must subtract out the noise bias from the power spectrum estimators with the filters defined in Eq. (81).

Recalling the discussion of the filters in Sec. IV B, we can eliminate Gaussian noise bias as well as noise-correlation between differing L by defining nonoverlapping filters sets (f_l^1,f_l^2) and (f_l^3,f_l^4). The resulting estimates of the deflection field d_{LM}^{12} and d_{LM}^{34} would then have statistically independent Gaussian noise properties such that the noise bias is eliminated in their cross correlation. Furthermore, if the signal is really due to lensing the various estimates of the deflection power spectrum must agree within their errors.

The price of dividing up the sample in this way is a reduction of the signal-to-noise in any given set. For example, by bandlimiting the filters of Eq. (81) to $500<l<1400$ for the (12) set and $l>1400$ for the (34) set, the total signal-to-noise is reduced by $\sim\sqrt{2}$ and correspondingly the errors in Fig. 1 are increased by $\sim\sqrt{2}$. Note that in this case, the underlying filtered temperature maps contain no power in the multipoles of interest $L\sim100$. Such a scheme would still yield a highly significant detection and help protect against

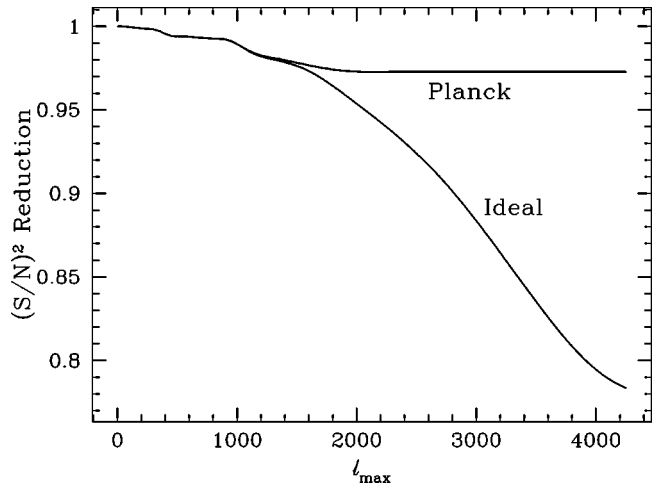

FIG. 5. Degradation in the total $(S/N)^2$ in the power spectrum due to covariance from gravitational lensing. The degradation is minimal for the Planck experiment or any that is cosmic variance limited only out to $l\sim 2000$.

contaminants. Filtered versions of other quadratic statistics can also serve as consistency checks. For example, even the simple temperature-temperature s statistic of Sec. IV C yields a $(S/N)^2\sim 200$ once it is is filtered according to the peaks in Fig. 2.

E. Power spectrum covariance

One might worry that the high signal-to-noise in the trispectrum for lensing comes at the expense of degraded signal-to-noise in the power spectrum due to covariance between the estimators. Fortunately this is not the case in the $l\lesssim 1000$ regime of the acoustic peaks. From Eqs. (34)–(36), we can calculate the degradation in the total $(S/N)^2$. This degradation is shown in Fig. 5 for the Planck satellite and an ideal experiment out to $l_{\rm max}$.

VI. DISCUSSION

We have provided a systematic study of the angular trispectrum or four-point function of the CMB temperature field. Symmetry considerations dictate the fundamental form of the trispectrum and govern the Gaussian noise properties of its estimators. The large number of independent configurations of the trispectrum imply that even subtle physical effects may be detectable when all of the information in the trispectrum is brought to bear.

In practice, extracting all of the information in the trispectrum will be a difficult computational task. We have thus also conducted a systematic study of the power spectra of quadratic statistics which probes different aspects of the trispectrum. Techniques developed for extracting power spectrum statistics from large data sets can then be brought to bear on the four-point function. The drawback is that this compression of information is in general a lossy procedure. We have therefore examined a wide range of quadratic statistics and prefiltering schemes. Given a target form for the trispectrum signal, these statistics can be optimized in their signal-to-noise for the power spectra.

As an example, we have reconsidered the four-point correlation generated by weak lensing of the primary anisotropies by the large-scale structure in the Universe as a means of recovering the power spectrum of the deflection angles or convergence [10]. CMB weak lensing provides a unique probe of the large-scale properties of the convergence field. We identify a specific quadratic statistic, the divergence of the temperature-weighted gradient field, that achieves the maximal signal-to-noise in this limit. For the Planck satellite, the total $(S/N)^2\approx 4000$ and represents a reduction in the noise variance on the convergence power spectrum by over an order of magnitude as compared with the gradient-gradient estimators of Ref. [10]. There is sufficient signal-to-noise to conduct filtering tests to eliminate noise bias and check for consistency between multipole subsets of the data. We plan to explore further the properties of these estimators and their use in extracting cosmological parameters in a separate work.

The lensing example illustrates the importance of examining the configuration properties of the trispectrum when designing statistical estimators based on the four-point function. Extracting the wealth of information potentially buried in the trispectrum will be a rich field for future studies.

ACKNOWLEDGMENTS

I thank A.R. Cooray and M. Zaldarriaga for many useful discussions. This work was supported by NASA ATP NAG5-10840 and the Sloan Foundation.

APPENDIX A: WIGNER-6j SYMBOL

1. Useful properties

The Wigner-6j symbol expresses the relationship between two distinct couplings of three angular momenta,

$$\begin{aligned}\mathbf{J}_d&=\mathbf{J}_a+\mathbf{J}_b+\mathbf{J}_c\\&=\mathbf{J_e}+\mathbf{J_c}\\&=\mathbf{J_a}+\mathbf{J_f},\end{aligned}\tag{A1}$$

such that the eigenstates of the (ec) coupling are related to the eigenstates of the (af) coupling as

$$|(ec)d\gamma\rangle=|(af)d\gamma\rangle\sqrt{(2e+1)(2f+1)}(-1)^{\Sigma}\begin{Bmatrix}a & b & e\\ c & d & f\end{Bmatrix},\tag{A2}$$

where $\Sigma\equiv a+b+c+d$. Geometrically, the Wigner 6j represents a quadrilateral with sides (a,b,c,d) whose diagonals form the triangles (a,d,f), (b,c,f), (c,d,e), and (a,b,e) or the three dimensional tetrahedron composed of these four triangles. It vanishes if the any of the triplets fail to satisfy the triangle rule. The symmetries are related to rotations of the tetrahedron that interchange the vertices. The result is that the symbol is invariant under the interchange of any two columns and under the interchange of the upper and lower arguments in any two columns.

The Wigner-6j symbol can thus be used to permute the pairings in a set of Wigner-3j symbols

$$\sum_f (2f+1)(-1)^{\Sigma+f-e-\alpha-\gamma}\begin{Bmatrix} a & b & e \\ c & d & f \end{Bmatrix}\begin{pmatrix} b & c & f \\ \beta & \gamma & -\phi \end{pmatrix} \times\begin{pmatrix} a & f & d \\ \alpha & \phi & -\delta \end{pmatrix}=\begin{pmatrix} a & b & e \\ \alpha & \beta & -\epsilon \end{pmatrix}\begin{pmatrix} e & c & d \\ \epsilon & \gamma & -\delta \end{pmatrix}, \tag{A3}$$

or equivalently by the orthogonality relation of the Wigner-3j symbols

$$\begin{Bmatrix} a & b & e \\ c & d & f \end{Bmatrix}=\sum_{\alpha\beta\gamma}\sum_{\delta\epsilon\phi}(-1)^{e+f+\epsilon+\phi}\begin{pmatrix} a & b & e \\ \alpha & \beta & \epsilon \end{pmatrix} \times\begin{pmatrix} c & d & e \\ \gamma & \delta & -\epsilon \end{pmatrix}\begin{pmatrix} a & d & f \\ \alpha & \delta & -\phi \end{pmatrix}\begin{pmatrix} c & b & f \\ \gamma & \beta & \phi \end{pmatrix}. \tag{A4}$$

Finally, the Wigner-6j symbol obeys

$$\sum_e (2e+1)\begin{Bmatrix} a & b & e \\ c & d & f \end{Bmatrix}\begin{Bmatrix} a & b & e \\ c & d & g \end{Bmatrix}=\frac{\delta_{fg}}{2f+1}, \tag{A5}$$

and

$$\sum_e (-1)^{e+f+g}(2e+1)\begin{Bmatrix} a & b & e \\ c & d & f \end{Bmatrix}\begin{Bmatrix} a & b & e \\ d & c & g \end{Bmatrix} =\begin{Bmatrix} a & c & g \\ h & d & f \end{Bmatrix}. \tag{A6}$$

2. Evaluation

Closed form expressions exist for special cases of the arguments. For example,

$$\begin{Bmatrix} a & b & e \\ c & d & 0 \end{Bmatrix}=\frac{(-1)^{a+b+e}}{\sqrt{(2a+1)(2b+1)}}\delta_{a,d}\delta_{b,c}. \tag{A7}$$

More generally, they may be computed efficiently by a recursive algorithm introduced in Ref. [16]. Let us define

$$h(j_1)=\begin{Bmatrix} j_1 & j_2 & j_3 \\ l_1 & l_2 & l_3 \end{Bmatrix}. \tag{A8}$$

The $h(j_1)$ satisfy the recursion

$$j_1E(j_1+1)h(j_1+1)+F(j_1)h(j_1)+(j_1+1)E(j_1)h(j_1-1)=0, \tag{A9}$$

where

$$E(j_1)=\{[j_1^2-(j_2-j_3)^2][(j_2^2+j_3^2+1)^2-j_1^2][j_1^2-(l_2-l_3)^2] \times[(l_2+l_3+1)^2-j_1^2]\}^{1/2},$$

$$F(j_1)=(2j_1+1)\{j_1(j_1+1)[-j_1(j_1+1)+j_2(j_2+1)+j_3(j_3+1)]+l_2(l_2+1)[j_1(j_1+1)+j_2(j_2+1)-j_3(j_3+1)]-l_3(l_3+1)[j_1(j_1+1)-j_2(j_2+1)+j_3(j_3+1)]-2j_1(j_1+1)l_1(l_1+1)\}. \tag{A10}$$

For a stable recursion, one begins at both of the two ends $j_{1\min}=\max(|j_2-j_3|,|l_2-l_3|)$ $j_{1\max}=\min(j_2+j_3,l_2+l_3)$ with the boundary conditions $E(j_{1\min})=0$ and $E(j_{1\max}+1)=0$ and matches the two in the middle.

The normalization is fixed by

$$\sum_{j_1}(2j_1+1)(2l_1+1)[h(j_1)]^2=1,$$

$$\mathrm{sign}[h(j_{1\max})]=(-1)^{j_2+j_3+l_2+l_3}, \tag{A11}$$

which follow from Eq. (A5).

APPENDIX B: FLAT-SKY APPROXIMATION

In the flat-sky approximation, one decomposes the temperature field into Fourier harmonics

$$\langle\Theta(\hat{\mathbf{n}}_1)\cdots\Theta(\hat{\mathbf{n}}_n)\rangle=\int\frac{d^2l_1}{(2\pi)^2}\cdots\int\frac{d^2l_n}{(2\pi)^2}\langle\Theta(\mathbf{l}_1)\cdots\Theta(\mathbf{l}_n)\rangle e^{i\mathbf{l}\cdot\hat{\mathbf{n}}_1}\cdots e^{i\mathbf{l}\cdot\hat{\mathbf{n}}_2}. \tag{B1}$$

Statistical isotropy is enforced by demanding that the correlation function be invariant under an arbitrary translation and rotation in the plane. Parity invariance is enforced by demanding symmetry under inversion of the coordinates or reflection across one of the coordinate axes.

As usual translational symmetry $\hat{\mathbf{n}}_i\to\hat{\mathbf{n}}_i+\mathbf{C}$, where $\mathbf{C}$ is a constant vector, is enforced by the closure condition that the n-point function is proportional to

$$(2\pi)^2\delta(\mathbf{l}_1+\cdots+\mathbf{l}_n). \tag{B2}$$

The wave vectors $\mathbf{l}_i$ thus form a geometric figure of n, possibly intersecting, sides. Rotational invariance for the two-point function and rotational and parity invariance for the three-point function imply that the corresponding harmonic spectra are functions only of the lengths of the sides:

$$\langle\Theta(\mathbf{l}_1)\Theta(\mathbf{l}_2)\rangle=(2\pi)^2\delta(\mathbf{l}_{12})C_{(l_1)}, \qquad \langle\Theta(\mathbf{l}_1)\Theta(\mathbf{l}_2)\Theta(\mathbf{l}_3)\rangle=(2\pi)^2\delta(\mathbf{l}_{123})B_{(l_1,l_2,l_3)}, \tag{B3}$$

where $\mathbf{l}_{i\cdots j}\equiv\mathbf{l}_i+\cdots+\mathbf{l}_j$ and B should be symmetric against permutations of its arguments. For the four-point function, rotational and parity invariance implies that the quadrilateral formed by the four wave vectors is a function of the lengths of the sides and the lengths of the two diagonals,

$$\langle \Theta(\mathbf{l}_1)\cdots\Theta(\mathbf{l}_4)\rangle = (2\pi)^4[\,\delta(\mathbf{l}_{12})\delta(\mathbf{l}_{34})C_{l_1}C_{l_2} + \delta(\mathbf{l}_{13})\delta(\mathbf{l}_{24})C_{l_1}C_{l_3} + \delta(\mathbf{l}_{14})\delta(\mathbf{l}_{23})C_{l_1}C_{l_4}] + (2\pi)^2\delta(\mathbf{l}_{1234})T^{(l_1,l_2)}_{(l_3,l_4)}(l_{12},l_{13}). \tag{B4}$$

To parallel our treatment of the all-sky four-point function, let us break Q into its three distinct pairings and demand symmetry with respect to permutation of the arguments,

$$T^{(l_1,l_2)}_{(l_3,l_4)} = P^{(l_1,l_2)}_{(l_3,l_4)}(l_{12}) + P^{(l_1,l_3)}_{(l_2,l_4)}(l_{13}) + P^{(l_1,l_4)}_{(l_3,l_2)}(l_{14}). \tag{B5}$$

Note that l_{14} is a function of the other two diagonals. P is symmetric under interchange of its upper and lower arguments as well as ordering within them.

The relationship between the all-sky and flat sky spectra can be obtained by noting that [7]

$$\Theta_{lm} = i^m\sqrt{\frac{2l+1}{4\pi}}\int\frac{d\phi_{\mathbf{l}}}{2\pi}e^{im\phi_{\mathbf{l}}}\Theta(\mathbf{l}),$$

$$\delta(\mathbf{l}_{i\ldots j}) = \int\frac{d\hat{\mathbf{n}}}{(2\pi)^2}e^{i\mathbf{l}_{i\cdots j}\cdot\hat{\mathbf{n}}},$$

$$e^{i\mathbf{l}\cdot\hat{\mathbf{n}}} = \sqrt{\frac{2\pi}{l}}\sum_m i^m Y_l^m(\hat{\mathbf{n}})e^{im\phi_{\mathbf{l}}}, \tag{B6}$$

where $\phi_{\mathbf{l}}$ is the polar angle of $\mathbf{l}$. It is a straightforward exercise to show that

$$C_l = C_{(l)},$$

$$B_{l_1l_2l_3} = \begin{pmatrix} l_1 & l_2 & l_3 \\ 0 & 0 & 0 \end{pmatrix} \times\sqrt{\frac{(2l_1+1)(2l_2+1)(2l_3+1)}{4\pi}}B_{(l_1,l_2,l_3)}. \tag{B7}$$

For the trispectrum, we begin with the general correspondence

$$\langle\Theta_{l_1m_1}\cdots\Theta_{l_4m_4}\rangle_c = \left(\prod_{i=1,4}\sqrt{\frac{l_1}{2\pi}}\int\frac{d\phi_{\mathbf{l_i}}}{2\pi}e^{-im_i\phi_{\mathbf{l}_i}}\right)\times(2\pi)^2\delta(\mathbf{l}_{1234})T^{(l_1,l_2)}_{(l_3,l_4)}(l_{12}), \tag{B8}$$

where "c" denotes the subtraction of the Gaussian piece in Eq. (B4). We then exploit the pair symmetry of the trispectrum exhibited in Eq. (B5) by breaking the delta function into the corresponding pairs. For the (12), (34) pairing,

$$\delta(\mathbf{l}_{1234}) = \int d^2L\,\delta(\mathbf{l}_1+\mathbf{l}_2+\mathbf{L})\,\delta(\mathbf{l}_3+\mathbf{l}_4-\mathbf{L}), \tag{B9}$$

such that $L = l_{12}$. Expanding the delta functions in spherical harmonics,

$$\delta(\mathbf{l}_{1234}) = \frac{1}{(2\pi)^2}\sum_{m_1\cdots m_4}\sum_{LM}\left(\prod_{i=1,4}\sqrt{\frac{2\pi}{l_i}}e^{im_i\phi_{\mathbf{l}_i}}\right)\frac{2L+1}{4\pi} \times\sqrt{(2l_1+1)\cdots(2l_4+1)}\begin{pmatrix} l_1 & l_2 & L \\ 0 & 0 & 0 \end{pmatrix} \times\begin{pmatrix} l_3 & l_4 & L \\ 0 & 0 & 0 \end{pmatrix}(-1)^M\begin{pmatrix} l_1 & l_2 & L \\ m_1 & m_2 & M \end{pmatrix} \times\begin{pmatrix} l_3 & l_4 & L \\ m_3 & m_4 & -M \end{pmatrix}. \tag{B10}$$

Substituting back in and integrating over the polar angles, we obtain the general correspondence

$$P^{l_1l_2}_{l_3l_4}(L) = \frac{2L+1}{4\pi}\sqrt{(2l_1+1)\cdots(2l_4+1)}\begin{pmatrix} l_1 & l_2 & L \\ 0 & 0 & 0 \end{pmatrix} \times\begin{pmatrix} l_3 & l_4 & L \\ 0 & 0 & 0 \end{pmatrix}P^{(l_1,l_2)}_{(l_3,l_4)}(L), \tag{B11}$$

from which we can construct the relation for $T^{l_1l_2}_{l_3l_4}$.

We can now also make the correspondence between the signal-to-noise in the all-sky and flat-sky formalisms. The weighting of four-point terms that maximizes the signal-to-noise is [6]

$$\left(\frac{S}{N}\right)^2_{\rm tot} = \frac{f_{\rm sky}}{\pi}\frac{1}{24}\frac{1}{(2\pi)^4}\int d^2\mathbf{l}_1\int d^2\mathbf{l}_2\int d^2\mathbf{l}_3\int d^2\mathbf{l}_4\,\delta(\mathbf{l}_{1234}) \times\frac{|T^{(l_1,l_2)}_{(l_3,l_4)}|^2}{C^{\rm tot}_{l_1}C^{\rm tot}_{l_2}C^{\rm tot}_{l_3}C^{\rm tot}_{l_4}}, \tag{B12}$$

where $f_{\rm sky}$ is the fraction of sky covered by the sample.

The square of T in this expression contains cross terms in the P pairings,

$$\left(\frac{S}{N}\right)^2_{\rm tot} = \left(\frac{S}{N}\right)^2_{(12,12)} + \left(\frac{S}{N}\right)^2_{(13,13)} + \left(\frac{S}{N}\right)^2_{(14,14)} + 2\left(\frac{S}{N}\right)^2_{(12,13)} + 2\left(\frac{S}{N}\right)^2_{(12,14)} + 2\left(\frac{S}{N}\right)^2_{(13,14)}. \tag{B13}$$

The correspondence with the all-sky expression, Eq. (33), can be established by considering the terms pair by pair. For

example for the (12), (13) term, one expands the delta function in the (12), (34) pairing as above and inserts an additional delta function

$$\pi\delta(\mathbf{l}_{1234}) = \pi \int d^2L_{13}\delta(\mathbf{l}_1+\mathbf{l}_3-\mathbf{L}_{13})\,\delta(\mathbf{l}_2+\mathbf{l}_4+\mathbf{L}_{13}), \tag{B14}$$

with the understanding that $\delta(\mathbf{0}) = V/(2\pi)^2 = 1/\pi$. Expanding the delta functions in spherical harmonics we can integrate over azimuthal angles to obtain

$$\left(\frac{S}{N}\right)^2_{(12,13)} = \frac{f_{\rm sky}}{24} \sum_{l_1 m_1 \cdots l_4 m_4} \sum_{L_{12} M_{12}} \sum_{L_{13} M_{13}} (-1)^{M_{12}+M_{13}} \times \begin{pmatrix} l_1 & l_2 & L_{12} \\ m_1 & m_2 & M_{12} \end{pmatrix} \begin{pmatrix} l_3 & l_4 & L_{12} \\ m_3 & m_4 & -M_{12} \end{pmatrix} \times \begin{pmatrix} l_1 & l_3 & L_{13} \\ m_1 & m_3 & M_{13} \end{pmatrix} \begin{pmatrix} l_2 & l_4 & L_{13} \\ m_2 & m_4 & -M_{13} \end{pmatrix} \times \frac{P^{l_1 l_2^*}_{l_3 l_4}(L_{12}) P^{l_1 l_3}_{l_2 l_4}(L_{13})}{C^{\rm tot}_{l_1} C^{\rm tot}_{l_2} C^{\rm tot}_{l_3} C^{\rm tot}_{l_4}},$$

$$= \frac{f_{\rm sky}}{24} \sum_{l_1 \cdots l_4} \sum_{L_{12} L_{13}} (-1)^{l_2+l_3} \begin{Bmatrix} l_1 & l_2 & L_{12} \\ l_4 & l_3 & L_{13} \end{Bmatrix} \frac{P^{l_1 l_2 *}_{l_3 l_4}(L_{12}) P^{l_1 l_3}_{l_2 l_4}(L_{13})}{C^{\rm tot}_{l_1} C^{\rm tot}_{l_2} C^{\rm tot}_{l_3} C^{\rm tot}_{l_4}}, \tag{B15}$$

where we have used Eq. (A4) to rewrite the sum over the Wigner-3j symbols in terms of the 6j-symbol. Proceeding similarly for all terms in the signal-to-noise expression, we obtain

$$\left(\frac{S}{N}\right)^2_{\rm tot} = \frac{f_{\rm sky}}{24} \sum_L \sum_{l_1 l_2 l_3 l_4} \frac{1}{2L+1} \frac{|T^{l_1 l_2}_{l_3 l_4}(L)|^2}{C^{\rm tot}_{l_1} C^{\rm tot}_{l_2} C^{\rm tot}_{l_3} C^{\rm tot}_{l_4}}, \tag{B16}$$

where we have employed Eq. (A6) to reexpress the (13), (14) term. The factor of 24 comes from the 4! permutations of each quadruplet in the all-sky expression. The $f_{\rm sky}$ term is the reduction in signal-to-noise due to incomplete skycoverage.

[1] D.M. Goldberg and D.N. Spergel, Phys. Rev. D **59**, 103002 (1999).
[2] U. Seljak and M. Zaldarriaga, Phys. Rev. D **60**, 043504 (1999).
[3] A.R. Cooray and W. Hu, Astrophys. J. **534**, 533 (2000).
[4] T. Falk, R. Rangarajan, and M. Srednicki, Astrophys. J. Lett. **403**, L1 (1993); X. Luo and D.N. Schramm, Phys. Rev. Lett. **71**, 1124 (1993); A. Gangui, F. Lucchin, S. Matarrese, and S. Mollerach, Astrophys. J. **430**, 447 (1994).
[5] X. Luo, Astrophys. J. **427**, 71 (1994).
[6] M. Zaldarriaga, Phys. Rev. D **62**, 063510 (2000).
[7] W. Hu, Phys. Rev. D **62**, 043007 (2000); the relation between ϕ and Φ or κ has the wrong sign.
[8] D.N. Spergel and D.M. Goldberg, Phys. Rev. D **59**, 103001 (1999).
[9] E. Newman, and R. Penrose, J. Math. Phys. **7**, 863 (1966); J.N. Goldberg *et al.*, *ibid.* **8**, 2155 (1967).
[10] M. Zaldarriaga and U. Seljak, Phys. Rev. D **59**, 123507 (1999).
[11] U. Seljak, Astrophys. J. **463**, 1 (1996).
[12] M. Zaldarriaga and U. Seljak, Phys. Rev. D **58**, 023003 (1998).
[13] R.B. Metcalf and J. Silk, Astrophys. J. **489**, 1 (1997).
[14] See http://astro.estec.esa.nl/SA-general/Projects/Planck; we take the inverse-variance weighted noise as in Ref. [3].
[15] W. Hu astro-ph/0108090.
[16] K. Schulten and R. Gordon, J. Math. Phys. **16**, 1971 (1975).